INSTITUTE OF PHYSICS PUBLISHING CLASSICAL AND QUANTUM GRAVITY

Class. Quantum Grav. **19** (2002) 1793–1801 PII: S0264-9381(02)29459-9

Method for compensation of thermally induced modal distortions in the input optical components of gravitational wave interferometers

Guido Mueller, Rupal S Amin, Dave Guagliardo, Donovan McFeron, Ramsey Lundock, David H Reitze and D B Tanner

Department of Physics, University of Florida, Gainesville, FL 32611-8440, USA

E-mail: mueller@phys.ufl.edu

Received 4 October 2001, in final form 17 January 2002
Published 18 March 2002
Online at stacks.iop.org/CQG/19/1793

Abstract

The next generation of interferometric gravitational wave detectors will employ laser powers approaching 200 W to increase shot-noise limited sensitivity. Optical components that transmit the laser light will exhibit increased thermal lensing induced by bulk absorption and concomitant changes in the material refractive index, resulting in significant changes in the modal characteristics of the beam. Key interferometer components such as electro-optic modulators and Faraday isolators are particularly at risk, since they possess relatively large absorption coefficients. We present a method for passive correction of thermally induced optical path length ($\Delta\Lambda$) changes induced by absorption in transmissive optical components. Our method relies on introducing material in the optical path that possesses a negative index temperature derivative, thereby inducing a compensating opposite $\Delta\Lambda$. We experimentally demonstrate a factor of 10 reduction in higher order spatial mode generation for terbium gallium garnet, a Faraday isolator material.

PACS number: 0480N

1. Introduction

A worldwide network of interferometers will soon begin to search for gravitational radiation [1–4]. Nevertheless, even the most optimistic estimation of event rates for the most likely astrophysical candidate source, binary inspirals, falls below one per year given the design sensitivities of these detectors. Thus, the Laser Interferometer Gravitational Wave Observatory (LIGO) plans to upgrade its detectors (Advanced LIGO) by implementing a variety of changes designed to increase strain sensitivity by more than an order of magnitude [5]. One of the major changes will be an increase in the input power up to 180 W for high-frequency

signals. This increased power has profound consequences for the input optical components in LIGO. Key optical components such as electro-optic modulators and Faraday isolators will experience severe thermal distortions due to their relatively large absorption ($\approx$1%). If we consider a Gaussian beam propagating through a slightly absorptive substrate, a radial temperature gradient will form in the substrate that modifies the temperature-dependent index of refraction. The indices of refraction of most optical materials increase with increasing temperature, resulting in the formation of a positive lens. The spherical part of the lens will focus the beam and change the mode matching into the main interferometer. The non-spherical part introduces higher order spatial modes that cannot be mode matched to the interferometer with simple curved mirrors or lenses. As we will show later, if we assume a mode matching of 100% at 0 W input power, the mode matching could be reduced to less than 10% at 180 W. Including the spherical part into the mode matching calculation would recover about 60% of the light. The residual 40% will be in higher order modes which do not resonate inside the arm cavities. These modes will increase the noise floor on all photo detectors and the loss will reduce the shot-noise limited sensitivity by about 23%. Light in higher order modes will scatter back into the fundamental mode inside the interferometer. This introduces increased offsets on feedback loops and subsequent increases in the sensitivity to technical noise sources. In addition, the Advanced LIGO interferometer is designed to have at least two operating points (20 and 180 W) to optimize detection of different astrophysical phenomena. As a result changing to 20 W input power to target low-frequency gravitational waves would require unacceptably large changes in the positions of various input optics.

In this paper we present a method for suppressing thermally induced modal distortions through the use of a compensating optical component. The theory, practical issues and first experimental results will be discussed. The idea behind the method is conceptually quite simple. It is possible to find transmissive optical materials whose indices of refraction *decrease* with increasing temperature, offering the possibility of restoring the modal purity by introducing a matched non-spherical negative lens. In principle, this technique can be applied to many optical components. In fact, a comparable configuration was independently developed by Graf *et al* [6] for intra-cavity use in Nd:YAG lasers. In Advanced LIGO this technique will allow for high-power propagation through critical optical components such as Faraday isolators (FIs) and electro-optic modulators (EOM) with minimal modal distortion.

2. Thermal effects in long optical crystals

Long optical crystals are found primarily in two locations prior to entering LIGO's core optics. These are the electro-optic modulators (EOM) and the Faraday isolators (FI). EOM are used to modulate the phase of the laser to generate sidebands adjacent to the laser frequency. These sidebands are used in LIGO for sensing the positions of the mirrors to lock the interferometer. EOM are based on the electro-optic effect and require electro-optic active crystals such as lithium niobate ($LiNbO_3$), potassium titanyl arsenate (KTA) or rubidium titanyl phosphate (RTP). The modulators are located on the optical table in air in front of the vacuum suspended mode cleaner. The FI prohibits light that is reflected at the core optic from re-entering the mode cleaner and the pre-stabilized laser. Optical isolators are based on the Faraday effect and require a magneto-optically active glass or crystal such as terbium gallium garnet (TGG). While the constituent materials for both EOM and FI will experience significant thermal lensing, TGG has a larger absorption coefficient compared to most electro-optic crystals. Moreover, its location after the mode cleaner but before the main interferometer means that its effects are more significant.

At low power levels, optical crystals behave in idealized fashions. They transmit light without modal aberration within the optic itself. When the power is increased, absorption of light heats the crystal causing thermal gradients. The thermal gradient can be found by integrating the thermal diffusion equation:

$$\nabla^2 T(\vec{r}) + \frac{q(\vec{r})}{k_{\text{th}}} = 0 \tag{1}$$

where $T(\vec{r})$ is the temperature, $q(\vec{r})$ is the heat source and k_{th} represents the thermal conductivity. In the case the system is cylindrically symmetric and the crystal diameter is much smaller than its length, the steady state heat flow is radial. The incoming laser mode can be approximated by a pure Gaussian (TEM_{00}) beam. The following solution can be obtained for the radial temperature profile:

$$\Delta T(r) = \frac{\alpha P}{4\pi k_{\text{th}}} \sum_{j=1}^{\infty} \frac{(-1)^j \left(2\frac{r^2}{w^2}\right)^j}{jj!} \tag{2}$$

where α is the absorption coefficient per unit length, P is the incident laser power, r is the radial coordinate and w is the TEM_{00} Gaussian beam radius.

The thermal gradient alters the optical path length through the temperature-dependent index of refraction, the thermally dependent photo-elastic effect and bulk expansion under heating. In most cases $\mathrm{d}n/\mathrm{d}T$ dominates and the spatial dependence of the differential optical path length $\Delta\Lambda(r)$ can be written as

$$\Delta\Lambda(r) = \frac{\mathrm{d}n}{\mathrm{d}T} L \Delta T(r). \tag{3}$$

Intuitively, we can imagine that it is possible to introduce a material possessing a negative $\mathrm{d}_n/\mathrm{d}T$ such that the total $\Delta\Lambda_{\text{tot}}$ is minimized:

$$\Delta\Lambda_{\text{tot}} = \Delta\Lambda_1 + \Delta\Lambda_2 = \frac{\mathrm{d}n_1}{\mathrm{d}T} L_1 \Delta T_1(r) + \frac{\mathrm{d}n_2}{\mathrm{d}T} L_2 \Delta T_2(r) = 0. \tag{4}$$

In this case, $\Delta\Lambda$ is constant and independent of radius; the beam will not observe the lens or any other degradation. A perfect compensation would be possible if the temperature profile in both materials has the same shape. This requires that the boundary conditions are similar and that the beam profile of the heating beam is the same in both materials, which in turn requires that the distance between the two materials is much smaller than the induced thermal lens and the Rayleigh range of the incoming laser mode. Note that it is not necessary to match the lengths of the crystals and the temperature dependence of the index of refraction. Only the products $\Delta T L(\mathrm{d}n/\mathrm{d}T)$ enter the equation and need to be matched.

3. Theoretical models

The laser mode is described as a fundamental Gaussian TEM_{00},

$$u_{00} = \sqrt{\frac{2}{\pi}} \frac{1}{w} \mathrm{e}^{-\frac{r^2}{w^2}} \tag{5}$$

with beam size w that is focused into the isolator (TGG) crystal. The change in the optical path length induces an additional phase shift across the beam profile:

$$u_{\text{aber}} = u_{00}\, \mathrm{e}^{\mathrm{i}2\pi \frac{\Delta\Lambda_1(r)}{\lambda}}. \tag{6}$$

This aberrated beam can be expanded in a set of cylindrical symmetric Laguerre–Gaussian eigenmodes u_{n0}:

$$u_{\text{aber}} = \sum_{n=0}^{\infty} c_n u_{n0} = \sum_{n=0}^{\infty} c_n L_n \left(2\frac{r^2}{w^2}\right) u_{00} \tag{7}$$

where L_n represent the Laguerre polynomials [7]. The coefficients c_n can numerically be obtained by evaluating the following integral:

$$c_n = 2\pi \int_0^{\infty} u_{n0}^*(r) u_{\text{aber}} r \, \mathrm{d}r. \tag{8}$$

During the propagation to the second crystal each Laguerre–Gauss mode is shifted in phase:

$$u'_{\text{aber}} = \sum_{n=0}^{\infty} c_n u_{n0} \, \mathrm{e}^{\mathrm{i}2n\Psi_g} \tag{9}$$

where Ψ_g is the Gouy phase between the two crystals: $\Psi_g = \text{atan}(L/z_R)$. The Rayleigh range $z_R = \pi w_0^2/\lambda$ depends on the beam waist w_0 of the original beam. In our experiments and in Advanced LIGO z_R is or will be in the 3 m range. This is much larger than the distance L between the crystals. Therefore the change in the beam size of the Laguerre–Gaussian modes during the propagation to the second crystal can be neglected. The second crystal imposes an additional phase shift of opposite sign onto the beam:

$$u_{\text{comp}} = u'_{\text{aber}} \, \mathrm{e}^{-\mathrm{i}2\pi \frac{\Delta\Lambda_2(r)}{\lambda}}. \tag{10}$$

The amount of light in the original mode is finally

$$P_{\text{co}} = \left| 2\pi \int_0^{\infty} u_{\text{comp}}^* u_{00} r \, \mathrm{d}r \right|^2. \tag{11}$$

For a vanishing Gouy phase Ψ_g, the original mode is perfectly reconstructed. In practice, it is important to ensure that the phase shift $2n\Psi_g$ for all Laguerre–Gauss modes with significant amplitude c_n is small. In this case the phase distortion in the first crystal has not changed the intensity profile before the beam enters the second crystal and the second crystal is able to reconstruct the beam.

A numerical model was developed to simulate the propagation of a laser mode through the two crystals. In this model, we truncated the infinite sum in equation (2) at $j = 201$ and included the first 18 Laguerre–Gauss modes in the analysis. The result from equation (11) is then compared with the intensity in the original mode without compensation (see equation (8)):

$$P_{\text{wo}} = |c_0|^2. \tag{12}$$

In addition, this compensation technique is compared with the case in which the spherical part of the thermal lens is simply included in the mode-matching calculation. For this we searched for the fundamental Gauss mode v_{opt} that has the largest overlap with the distorted beam:

$$P_{\text{fc}} = \left| 2\pi \int_0^{\infty} u_{\text{aber}}^* v_{\text{opt}} r \, \mathrm{d}r \right|. \tag{13}$$

The results for a TGG crystal with an ideal compensator crystal are shown together with the experimental results in figure 1. Without any compensation the power in the original TEM_{00} mode drops from 100% at 0 W to below 5% at 180 W. Only about 60% or 110 W can be

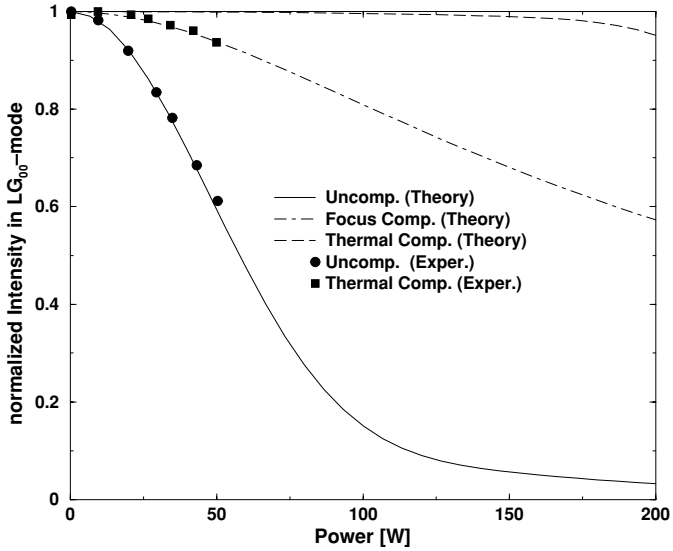

Figure 1. The intensity in the fundamental cavity eigenmode normalized to the intensity at 0 W pump power. The solid line shows the fast decay in the mode matching for uncompensated thermal lensing down to 5% at 150 W laser power. Parts of the power (68% at 150 W) can be recovered by including the spherical part of the thermal lens in a mode matching calculation (dot-dashed line). Nearly the full power (>98.8% at 150 W) can be recovered with a matched thermal compensation scheme. The experimental data for the uncompensated case (circles) follow the theoretical curve very well. The experimental data for the thermally compensated case (squares) only coincidentally follow the focus-compensated curve (see text and figure 3 for details). Note that neither the theory nor the experimental data include a fitting parameter. The size of the circles and squares represents the error bars of the intensity measurement.

recovered by optimizing the mode matching. For the ideal compensator placed in this example 3 cm behind the TGG crystal, 97.5% of the original mode is recovered.

A further reduction to 1.5 cm would increase the mode matching by an additional 1%. But there are certain practical limits such as the dimensions of the crystals itself, which are already included in the analysis. In addition, it might be necessary to place the compensator crystal in front of the input polarizer of the FI to avoid a decrease in the isolation ratio caused by thermally induced birefringence in the compensator crystal. In that case, the minimum distance is determined by the space the polarizer requires.

4. Experimental methods

Several practical problems must be solved before a compensator can reach its full potential. The first problem is to identify a suitable material with a negative $\mathrm{d}n/\mathrm{d}T$. We selected FK51 glass from Schott which has $\mathrm{d}n/\mathrm{d}T = -6 \times 10^{-6}\ \mathrm{K}^{-1}$. In addition, absorption coefficients can vary from sample to sample and it is virtually impossible to predetermine the exact length that is necessary to compensate the thermal lens perfectly. In our experiment (figure 1) we used two prisms to adjust the optical path length in the FK51. We note that in this case the compensating material is no longer cylindrical-symmetric and might overcompensate the thermal lens in one dimension and undercompensate in the second dimension due to non-radial heat flow.

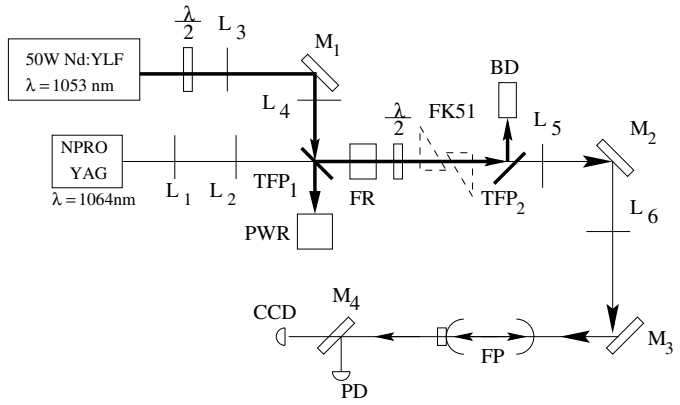

Figure 2. The experiment includes a 700 mW Nd:YAG non-planar ring oscillator (NPRO) which was focused via the lenses L_1 and L_2 into the Faraday isolator (FI). The FI was formed with the two thin film polarizers (TFP_1 and TFP_2), the Faraday rotator (FR) and the wave plate $\lambda/2$. The FK51 prisms were placed between the $\lambda/2$ plate and the TFP_2. The spatial mode of this laser was mode matched via L_3 and L_4 into the analyser cavity (FP). The transmitted signal was analysed with a photodetector (PD) and a CCD camera. The thermal lens was created with the 50 W Nd:YLF laser which was superimposed and mode matched to the Nd:YAG via L_5, L_6 and the thin film polarizer TFP_1. The second polarizer TFP_2 separated the two beams again. The power of the Nd:YLF in the interaction region was adjusted with a second $\lambda/2$ plate between the laser and L_5 controlled with the power meter PWR at the second output of TFP_1. $M_1, \ldots, M_4$ were some of the mirrors used to steer the laser beams. Most mirrors were omitted for clarity.

The modal composition of the laser field was analysed with a non-degenerate Fabry–Perot cavity in which different spatial modes have different resonance lengths. The transmitted signal was used to measure the power in each spatial mode while a CCD camera was used to identify the particular mode. This technique requires a frequency stable laser. We used a diode-pumped 700 mW Nd:YAG NPRO (350 mW in the interaction region) laser with intrinsic frequency stability which far exceeded our requirements. A 50 W Nd:YLF laser was used to create the thermal gradient in the crystals. Prior to the main measurements the intensity profiles of both lasers were measured with a two-axis beam scan and was found to have an M-value of about $M = 1.1$ with an ellipticity of less than 4%.

First we superimposed and mode matched both laser fields at the first polarizer, passed them through the Faraday rotator crystal (TGG) and a quartz rotator. The beams were separated again at the second polarizer. The beam size of both beams was about 1 mm. The intensity of the pump beam in the interaction region was adjusted with a half wave plate in front of the first polarizer. The probe beam was then mode matched and aligned into the analyser cavity. During the alignment we placed a quarter wave plate in front of the second polarizer. The subsequent rotation of polarization of pump and probe beam allowed both laser fields to be transmitted and reflected at the last polarizer. Both outputs were then used to superimpose the pump beam with the probe beam. Imperfect superposition of the two beams causes the probe beam to be deflected by the index gradient generated by the pump beam. The deflection can be calculated from a Taylor expansion of $\Lambda(r)$ along the direction of the displacement. To keep the intensity in the first-order Hermite–Gauss mode HG_{10} below 2% of the intensity of the fundamental mode at all power levels, the pump beam has to be superimposed with the probe beam within about 5% of the beam radius[1]. The intensities in all detectable spatial

[1] A misaligned pump beam (for example, displaced by x_0) will deflect the probe beam and cause the excitation of the first-order Hermite–Gauss mode HG_{10}. The amplitude of this mode can be approximated from a Taylor expansion of $\Lambda(r)$ along one axis at x_0.

Table 1. The parameters of the TGG crystal and the FK51 crystal.

Material	α (cm^{-1})[a]	k_{th} (W mK^{-1})[b]	dn/dT (10^{-6} K^{-1})[b]	L (mm)
TGG	6.3×10^{-3}	7.4	20	35
FK51	9.2×10^{-3}	0.9	−6	67

[a] The absorption coefficient of this particular TGG crystal was measured in our group. The absorption coefficient of the FK51 prisms is a fit to the data. From the internal transmittance, we anticipated an absorption coefficient of 8×10^{-3} cm^{-1}.
[b] The thermal conductivity and the derivative of the index of refraction were obtained from [10] for TGG and from the FK51 data sheet.

modes were recorded for different pump powers and confirmed that our alignment was within 5% of the beam radius. The power of the probe beam in front of the analyser cavity was measured with a power meter every time the pump power was changed. The changes in the power over the full measurement were below $\pm 1\%$ of the average power. Later we added the FK51 prisms, realigned the beam into the cavity and repeated the measurement.

5. Results and discussion

Experiments using only the TGG indicated a substantial thermal lensing at high pump powers. In first order mode mismatch shifts power from LG_{00} towards LG_{10} [9]. In figure 2, the intensity in the cavity eigenmode normalized to the value at 0 W pump power is plotted (filled circles) versus YLF incident power. The size of the circles approximates the accuracy of the measured data. The intensity in the cavity eigenmode dropped to 60% at 50 W pump power following nearly exactly the theoretical curve. Note that the measured data are not fitted to the theoretical curve. The parameters for the TGG crystal and the FK51 are shown in table 1.[2] The absorption coefficient of this particular crystal was measured as 6.3×10^{-3} cm^{-1}, which is about a factor 6 larger than anticipated based on our own measurements in other TGG samples and a factor 3 larger than the values found in the literature [10].

Data taken with the FK51 (filled squares) indicate an increase in the intensity of the fundamental mode at high pump powers. The intensity drops only to 93.6%. It is important to note that it only coincidentally follows the theoretical curve for focus compensation rather than the curve for perfect thermal compensation. This incomplete compensation is brought about by the excess absorption in the TGG and, consequently, insufficient path length in the FK51. Nevertheless, the measured data can also be explained if we assume that the path length is approximately 68% of that needed for complete compensation (see figure 3).

To verify that we do not compensate only the focus, we reoptimized the mode matching into the cavity for the partially compensated set-up and achieved a final mode matching of $(97 \pm 1)\%$. This would not be possible for the simple focus compensation technique, as for this technique 94% is already the maximum mode matching that can be achieved. This result also shows that the requirements on matching the compensator crystal to the isolator crystal might be relaxed. The remaining mismatch could at least in parts be compensated with a change of the mode matching. This trade-off between the possibility to change the mode matching for various power levels, remaining higher order modes, and the accuracy with which we are able to match the compensator crystal to the isolator crystal needs to be analysed in the future.

[2] The parameters for FK51 can be found in the FK51 data sheet (no 487845) from Schott Optical Glass.

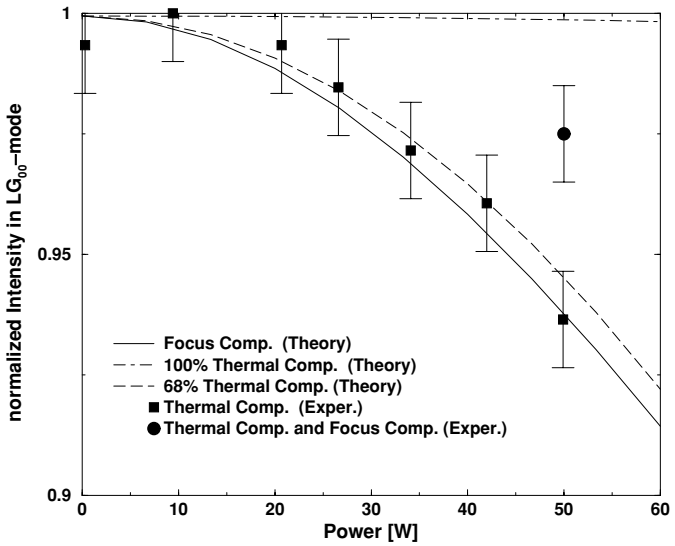

Figure 3. The intensity in the fundamental cavity eigenmode normalized to the intensity at 0 W pump power, except for the thermally compensated experimental data, where we used the larger value at 9 W pump power. The difference between the two data points is within the error bars of the experiment. The solid line shows the focus-compensated case. The dot-dashed line shows the intensity for matched (100%) compensation, while the dashed line shows the intensity for the case where the compensator crystal has only 68% of the optimum length. The experimental data (squares) could be explained by focus compensation or 68% thermal compensation. As we were able to increase the intensity in the fundamental mode of the cavity by changing the mode matching (circle), it is obvious that we were not focus compensated.

6. Conclusion

We have demonstrated a method for compensation of thermally induced modal distortions in Faraday isolators. Such a compensation scheme would permit Advanced LIGO to remain mode matched while changing the input power from low power during alignment times to intermediate power levels (20 W) for low-frequency gravitational wave searches to full power (180 W) for high-frequency searches without changing the mode matching for each power level. It would also reduce the amount of higher order modes far below the level possible with changes in the mode matching alone. Although we have shown its utility with Faraday isolators, it may also be applied to other transmissive optical components such as EOM crystals. Experiments are in progress to apply this technique to EOM materials, to utilize mode cleaning of the probe to increase the precision of our measurements and to increase the pump power to 100 W.

Acknowledgment

The authors gratefully acknowledge the support of the National Science Foundation through grant PHY-0070854.

References

[1] Abramovici A and the LIGO group 1992 LIGO: the Laser Interferometer Gravitational-Wave Observatory *Science* **256** 325–33

[2] Caron B and the VIRGO group 1997 The Virgo interferometer *Class. Quantum Grav.* **14** 1461

[3] Lueck H and the GEO 600 Team 1997 The GEO600 project *Class. Quantum Grav.* **14** 1471
[4] Kawabe K and the TAMA Collaboration 1997 Status of TAMA project *Class. Quantum Grav.* **14** 1477
[5] Gustafson E, Shoemaker D, Strain K and Weiss R 1999 LSC white paper on detector research and development *LIGO Document Center* T990080-00-D
[6] Graf Th, Wyss E, Roth M and Weber H P 2001 Laser resonator with balanced thermal lenses *Opt. Commun.* **190** 327–31
[7] Jeffrey A 1995 *Handbook of Mathematical Formulars and Integrals* (London: Academic) p 289
[8] Strain K A, Danzmann K, Mizuno J, Nelson P G, Rüdiger A, Schilling R and Winkler W 1994 Thermal lensing in recycling interferometric gravitational wave detectors *Phys. Lett.* A **194** 124–32
[9] Mueller G, Shu Q-Z, Adhikari R, Tanner D B, Reitze D, Sigg D, Mavalvala N and Camp J 2000 Determination and optimization of mode matching into optical cavities by heterodyne detection *Opt. Lett.* **25** 266–8
[10] Mansell J D, Hennawi J, Gustafson E K, Fejer M M, Byer R L, Clubley D, Yoshida S and Reitze D H 2001 Evaluating the effect of transmissive optic thermal lensing on laser beam quality with a Shack–Hartmann wave front sensor *Appl. Opt.* **40** 366–74